

Quantitative Measurement of Multifunctional Quantum Dot Binding to Cellular Targets Using Flow Cytometry

R. A. Smith, T. D. Giorgio*

Department of Biomedical Engineering,
Vanderbilt University, Nashville,
Tennessee

Received 9 March 2006; Revision
Received 16 October 2008; Accepted
20 October 2008

Grant sponsor: NIH; Grant number: 1R21
CA091299.

*Correspondence to: Todd D. Giorgio,
Vanderbilt University, Box 351620,
Station B, Nashville, TN 37235, USA.

Email: todd.d.giorgio@vanderbilt.edu

Published online 25 November 2008 in
Wiley InterScience (www.interscience.
wiley.com)

DOI: 10.1002/cyto.a.20677

© 2008 International Society for
Advancement of Cytometry

• Abstract

Semiconductor nanocrystals such as quantum dots (QDs) are a potentially powerful resource in the fields of flow cytometry and fluorescence microscopy. QD size and fluorescence characteristics offer attractive features for use in targeted delivery systems and detection by flow cytometry. While quantitative measurements of a variety of fluorescent molecules are routinely performed, fluorophores for which no calibration standards exist, such as QDs, pose a problem for quantitation in flow cytometry. Our goal was to develop a targeted nanoparticle delivery platform as well as a corresponding method to accurately and quantitatively assess the performance of this system. We synthesized surface-modified QD probes targeted to cellular surface receptors and measured the MFI of the resulting cell-probe conjugates by flow cytometry. MFI was converted to mean equivalent R-PE intensity (MEPE) using standard calibration microspheres. Known concentrations of both R-PE and QD probes were measured by fluorometry to relate R-PE and QD fluorescence. Fluorometry results were then used to translate MEPE measurements to the number of bound QD probes. The targeted probes exhibited superior binding characteristics over unmodified and untargeted particles. This binding interaction was shown to be specific and mediated by the NGR targeting peptide tethered to the QD surface. The calibration method developed to assess this system proved successful at converting raw fluorescence data to quantitative probe binding values. We demonstrate the synthesis and performance of a highly modular nanoparticle system capable of targeted binding and fluorescent imaging. The calibration method implemented to quantify the performance of this system represents a potentially powerful tool to utilize truly quantitative flow cytometry measurements with an array of fluorescent molecules, including QDs. © 2008 International Society for Advancement of Cytometry

• Key terms

flow cytometry; fluorometry; quantum dot; nanocrystal; quantitative; calibration; NGR; PEG

RECENT advances in library screening and other methods have identified new cell-specific surface markers potentially suitable for drug and gene delivery. The NGR tripeptide is one such molecule identified as a tumor-homing sequence that selectively targets tumor vasculature in vivo (1,2). Additional studies identified CD13 as the receptor for this peptide motif (3). CD13 expression has been reported in a variety of tissues, and a recent study has revealed the existence of at least two distinct isoforms of this antigen (4). Further investigation confirmed that the isoform found in tumorigenic cells and angiogenic blood vessels functions as a receptor for the NGR motif, while the isoform expressed in normal counterparts of these cells does not appreciably bind NGR conjugates. CD13 overexpression has been measured in both tumor cells and angiogenic blood vessels (5,6), providing an appealing and accessible target for directed therapy.

Molecules targeting receptors such as these have been incorporated into liposomes (7–9), microparticles and nanoparticles (10,11), and directly conjugated to drugs or genes (1,12,13) to facilitate delivery of high concentrations of therapeutic agents to the cell surface. The use of nanoparticles for this purpose has the inherent

advantage of a large surface area to volume ratio, allowing conjugation of multiple active molecules. Stable covalent conjugation of bioactive molecules such as enzymes (14,15), mAbs (16), peptides (17,18), and DNA (19,20) to the surface of NPs has been reported. With small-molecule ligands, short peptides, and DNA probes, multiple copies of the ligand can be attached to the surface of the quantum dot (QD) enabling multivalent binding to target cells.

QDs offer the typical characteristics of other nanoscale particles with the added benefit of intense fluorescence characteristics for straightforward and highly sensitive detection and imaging. These attributes impart the ability to integrate detection, imaging, and potential treatment characteristics (e.g. therapeutic payload delivery) into a single multifunctional nanoparticle. Particles such as these provide a stable and highly modular base for targeted delivery not offered by drugs or imaging materials alone. An intrinsic imaging capability enables detection and performance monitoring of these systems in a number of ways—fluorescence comparisons and analysis of small sample sizes can be accomplished in real time by fluorescence microscopy while more quantitative measurements and higher cell throughput can be performed by techniques such as flow cytometry. The current generation of QDs has been used successfully for both in vitro and small animal in vivo imaging (21,22). Nanomaterials currently in development aim to extend this capability by providing the potential for medical imaging with particles such as reduced-toxicity near-infrared (NIR) emitting QDs and other nanoparticulate contrast agents.

Traditional fluorophores (e.g., fluorescein isothiocyanate [FITC], R-phycoerythrin [R-PE], and enhanced green fluorescent protein [EGFP]) have been used extensively in conjunction with fluorescence microscopy and flow cytometry. Reliable fluorescence calibration standards have enabled users to move beyond basic sample detection and visualization to quantitative measurements utilizing these reagents (23–25). Unfortunately, many fluorescent molecules (including QDs) currently lack the necessary standards to facilitate quantitative approaches. Without suitable calibration methods, measurements are often limited to qualitative comparisons and relative fluorescence intensities (i.e., MFI) with little inherent connection to the biological structure or activity under assessment.

The calibration method employed in the current study shares some similarities with several previous works and is designed to extend the established body of work on quantitative flow cytometry. Typical quantitative calculations rely on standardized calibration microspheres for conversion of measured fluorescence intensity data to a measure of equivalent fluorophores (26–29). However, as many fluorophores, including QDs, lack these standards, alternative methods must be employed to facilitate their use in quantitative assays.

In this report we describe the synthesis and in vitro performance of a QD construct capable of multivalent targeted binding to cellular proteins and fluorescent labeling of targeted cells. These data provide a viable modular nanoscale platform capable of directed binding and delivery to target cells. Furthermore, we illustrate a method for fluorescence

calibration of flow cytometry data capable of extending quantitative measurement to these probes as well as to other fluorophores for which appropriate calibration standards are currently not available.

MATERIALS AND METHODS

Cell Culture

HT-1080 cells (human fibrosarcoma, ATCC CCL-121) were maintained and subcultured in complete medium consisting of minimum essential medium (MEM) consisting of 10% fetal bovine serum, 2 mM glutamine, 1.5 g/l sodium bicarbonate, 0.1 mM nonessential amino acids, 1 mM sodium pyruvate, and 1% antibiotics of penicillin-streptomycin-amphotericin. All cells were maintained at 37°C, 5% CO₂, and 95% humidity during the study. For probe binding assays, cells were grown to confluence in 12-well tissue culture plates containing 1 ml/well of supplemented MEM under the conditions described above.

Peptides and QD Probes

The cyclized PEGylated CD13-targeting peptide (HN-PEG-NGR) was synthesized and purified by AnaSpec (San Jose, CA), where HN-PEG is a 3400-Da PEG chain with functional groups suitable for subsequent synthesis reactions and NGR is the cyclized CNGRC targeting peptide. HN-PEG-NHS is the same PEG chain used in synthesis of the PEGylated CD13-targeting peptide described above and was obtained from Nektar Therapeutics (Huntsville, AL). The N-terminal amine group of the desired construct was conjugated to the surface of carboxylate QDs (585 nm emission; Quantum Dot Corp., Hayward, CA) using 1-ethyl-3-(3-dimethylaminopropyl)carbodiimide (EDC; Sigma) to produce QD-PEG and QD-PEG-NGR probes. Briefly, 250 μ l of QDs (7.5 μ M) was diluted to 1 μ M with 10 mM borate buffer, pH 7.4. Eighty microliters from a 10 mg/ml stock solution of HN-PEG-NHS or the HN-PEG-NGR targeting construct was then added to the solution. Fifty-seven microliters from a 10 mg/ml stock solution of EDC was added and the mixture was stirred for 2 h at room temperature to complete the conjugation.

Following conjugation, the mixture was purified by spin filtration in a 50,000 nominal molecular weight limit (NMWL) cutoff device (Amicon Ultra-4, Millipore Corp.). Three buffer exchanges were performed with 50 mM borate buffer (pH 8.3) and the final conjugate was stored at 4°C. The concentration of the final purified product was determined by measuring the absorbance at 575 nm using a QD extinction coefficient of 400,000 M⁻¹ cm⁻¹ (provided by QD Corp.). As this value is a characteristic of the semiconductor core, the extinction coefficient is presumably unchanged by surface functionalization. However, conjugation of molecules to the QD surface does have an effect on the fluorescence emission (i.e. quantum yield) of the final construct.

QD Probe Binding to Cellular Targets In Vitro

Ligand-target cell interactions were conducted in an in vitro cell culture model. Target HT-1080 cell samples were

grown to confluence in 12-well tissue culture plates before biological experimentation. QD-PEG-NGR solutions (50 or 100 nM) in OptiMEM supplemented with 1% BSA were introduced and incubated with cell samples for 1 h at 37°C on a shaker plate to promote convective transport of the targeted probes. Blocking studies followed the same protocol, with the addition of a 10-fold excess of soluble NGR added to the QD-PEG-NGR solution.

Following incubation and probe binding, QD solutions were aspirated and cell monolayers were washed three times with fresh PBS to remove any unbound QD probes. QD binding to adherent cells was then documented by fluorescence microscopy. Culture wells were treated with a nonenzymatic cell dissociation solution (Sigma) to detach the cell monolayer from the surface. The resulting samples were centrifuged for 5 min at 900g, resuspended in 500 μ l of fresh PBS, filtered through a 70- μ m mesh, and immediately analyzed by flow cytometry.

Photomicroscopy

The fluorescence of adherent HT-1080 cells following incubation with QD probes was documented by fluorescence microscopy. After washing the cell monolayer surface, phase contrast and corresponding fluorescence photomicrographs were taken of each experimental well. Samples were analyzed on a Nikon TE2000U inverted microscope using a fluorescence filter cube specifically designed for 585 nm emission QDs (Chroma Technology). Images were obtained with a Hamamatsu C7780 3 channel CCD cooled digital camera driven with Image-Pro Plus software (Media Cybernetics) and saved as individual JPEG files. Each experimental well was imaged at 10 \times magnification.

Quantification of QD Probe Binding

Flow cytometry. Fluorescence of all samples was measured on a FACSCalibur flow cytometer (Becton-Dickinson). CellQuest software (Becton-Dickinson) was used for all data acquisition. Cell-associated QD probe fluorescence as well as R-PE calibration microsphere emission was measured in the FL2 channel (band pass filter 585/42 nm). Data on forward scatter was collected in linear mode while all other parameters were collected in log mode. Twenty thousand events were collected by list-mode data for all samples, and the mean intensity (MFI) from the histograms for each sample was used to analyze their fluorescence intensity. WinList software (Verity Software House) was used to further prepare and analyze the list-mode data following collection.

For data acquisition, the cell region was determined by utilizing FSC and SSC measurements. Samples were then analyzed and the MFI of the FL2 channel was recorded for each sample. HT-1080 autofluorescence (from cells untreated with QD probes) was subtracted from these fluorescence intensities to arrive at a final measurement for further analysis. QuantumTM PE MESF microspheres (Bangs Labs) were analyzed by flow cytometry under the same conditions and settings used in biological experimentation.

Fluorometry. Fluorescence spectra of both QD probes and soluble R-PE were measured on an LS 50 B luminescence spectrometer (Perkin Elmer). For R-PE, 1667, 833.5, 250, 166.7, and 16.67 nM concentrations as well as blank PBS were measured in a small-volume quartz cuvette. Samples were excited at 488 nm (5-nm slit) and emission profiles were recorded from 564 to 606 nm (5-nm slit). Emission intensities for each sample were integrated to determine the total intensity within the measurement range (integrated intensity). A standard curve was then prepared relating R-PE concentration to measured integrated fluorescence intensity. QD probe fluorescence was measured using the same settings and the integrated intensity of these samples was compared to the standard curve to determine the equivalent number of R-PE molecules (i.e. the number of R-PE molecules required to equal the fluorescence of a QD probe).

Cross-correlation. R-PE calibration microspheres were used to correlate fluorescence measurements on the flow cytometer, producing a standard curve relating measured MFI to the number of equivalent R-PE molecules. The standard curve of calculated intensities from fluorometry was used to determine the number of R-PE molecules per QD probe. Using this comparison, a new standard curve was produced relating MFI measured by flow cytometry to the number of QD probes. This standard curve allows direct conversion of fluorescence measured by flow cytometry to the number of bound QD probes per cell in biological assays.

RESULTS

Probe Binding to Target Cells

Biologically active NGR cell-targeting peptides retain the capacity for specific binding to target cells after attachment to the QD surface. We tested the binding of QD-PEG-NGR conjugates to HT-1080 cells expressing high levels of the target CD13 receptor (Fig. 1A). Fluorescence photomicrographs revealed significant QD binding to target cells when the NGR targeting ligand was attached to the surface (Figs. 1C and 1D). This interaction is nearly completely inhibited by competitive binding with excess soluble NGR ligand (Figs. 1E and 1F).

Flow cytometry confirms the trends observed in the photomicrographs for these studies and yields data for quantitative analysis of binding interaction (Fig. 1B). A distinct increase in cellular FL2 fluorescence was noted after incubation with QD-PEG-NGR probes, indicating a strong interaction of the probe with the cellular surface. Control HT-1080 cells had a mean FL2 of 2.7 a.u. while those treated with the targeted QD probes had a mean intensity of 101.5 a.u. This shift in MFI suggests significant interaction of the probes with the cell surface, which can be further quantified by the calibration method described in this work.

Surface modification greatly influences QD association with the cell surface. Along with QD-PEG-NGR (mean intensity = 101.5 a.u.), we tested the binding of two other 50 nM solutions of QD probes (unmodified AMP QDs and QD-PEG) to target HT-1080 cells. Flow cytometry revealed markedly different interactions among each of these cohorts (Fig.

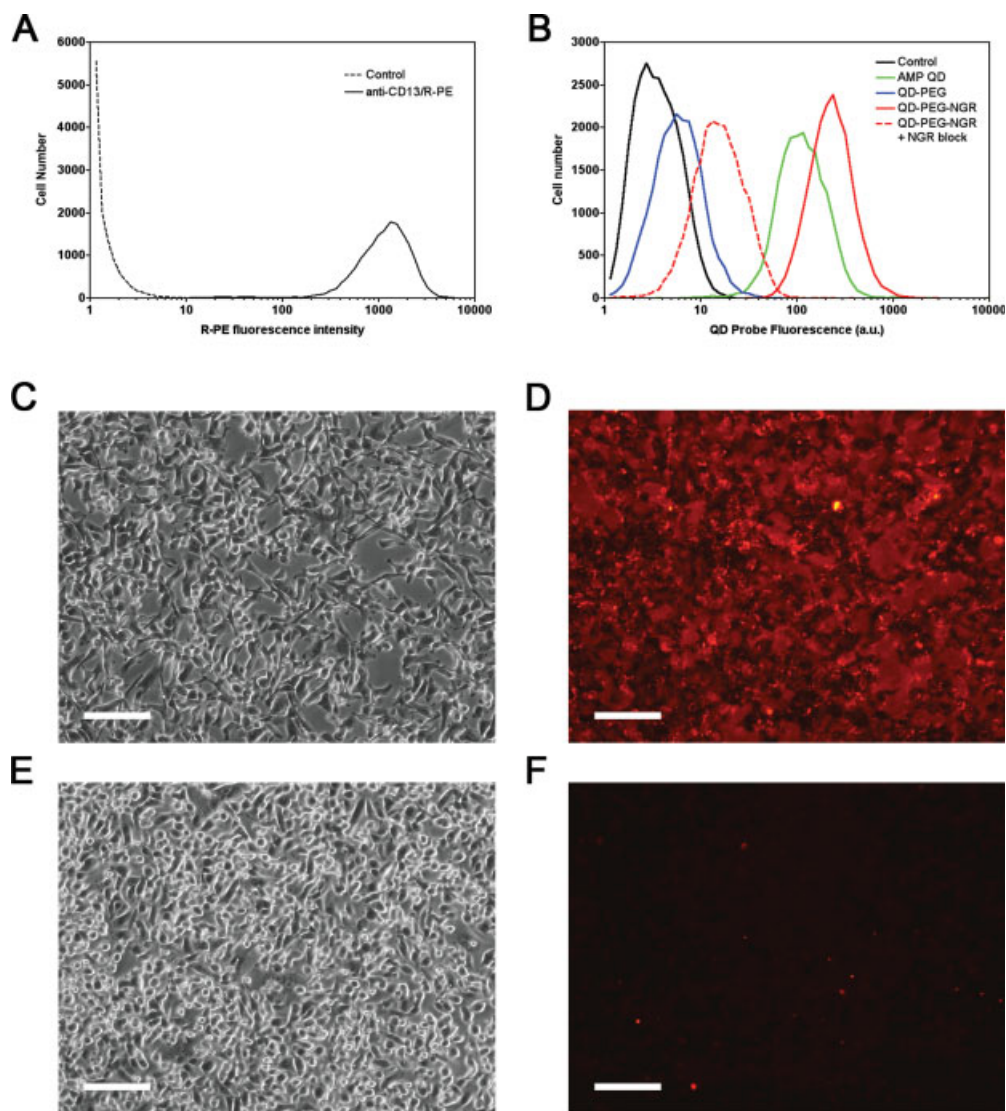


Figure 1. CD13-targeted molecules bind to the surface of HT-1080 cells. (A) HT-1080 cells express high levels of the CD13 protein on their surface. Incubation of the cells with an R-PE labeled anti-CD13 mAb (anti-CD13/R-PE) produces a unimodal cell population with an average FL2 intensity more than 1000-fold greater than that of untreated HT-1080 cells as measured by flow cytometry. (B) Surface modification influences QD probe interaction with HT-1080 cells as detected by flow cytometry. Control HT-1080 cells (black) exhibit low-level autofluorescence. QDs presenting the native AMP coating (green) are significantly associated with HT-1080 cells. The mechanism of unmodified QD association with cells is nonligand mediated based on the binding inhibition provided by PEG modification of the QD surface (blue). Addition of the NGR targeting ligand to the QD-PEG, producing the QD-PEG-NGR construct (solid red), regenerates extensive interaction with the cell surface. Nearly all of the NGR-mediated interaction can be blocked by coincubation of the cells with a 10-fold excess of free NGR ligand (dashed red), providing evidence for specificity of QD-PEG-NGR interaction with cells. Histograms are representative of $n \geq 3$ for all experimental cohorts. (C–F) Photomicrographs of QD probe association with HT-1080 cells. NGR surface functionalization specifically mediates QD binding. Images are representative of $n \geq 3$ for all experimental cohorts. (D) QDs functionalized with the NGR peptide interact extensively with the HT-1080 cell surface, resulting in a relatively high level of visible QD fluorescence in this photomicrograph. (F) Addition of 10-fold excess NGR ligand concurrently with QD-PEG-NGR inhibited nearly all QD interaction with the cell surface, greatly reducing detectable fluorescence. (C, E) Corresponding phase contrast images of cultured cells.

1B). HT-1080 cells had a mean intensity of 95.9 a.u. after incubation with unmodified AMP QDs, revealing considerable interaction of the amphiphilic polymer coating with the cell surface. This intensity fell to 3.6 a.u. (a 96% reduction) when the surface of the QDs was modified with PEG, demonstrating the ability of the PEG coating to mask recognition of the amphiphilic polymer surface.

The specificity of QD-PEG-NGR probe binding was further tested by competition with free NGR peptide. Introduction of a 10-fold excess of this ligand reduced the mean FL2 intensity from 101.5 to 11.5 a.u., an 89% reduction in probe binding to the cell surface. Addition of soluble BSA, however, had no effect on QD binding (data not shown). These results suggest that QD-PEG-NGR probe binding is modulated pri-

Table 1. Integrated intensities of QD probes and R-PE were measured by fluorometry to produce calibration standard curves (Fig. 2) for quantitative analysis

| | INTEGRATED FLUORESCENCE INTENSITY | RELATIVE BRIGHTNESS (COMPARED TO AMP QD) |
|-------------------|---|---|
| 500 nM AMP QD | 36547.6 | 1 |
| 250 nM AMP QD | 21230.1 | 1 |
| 125 nM AMP QD | 10407.3 | 1 |
| 75 nM AMP QD | 9207.7 | 1 |
| 62.5 nM AMP QD | 3725.7 | 1 |
| 1667 nM R-PE | 32568.0 | 0.24 |
| 833.5 nM R-PE | 15693.6 | 0.24 |
| 250 nM R-PE | 3731.5 | 0.24 |
| 166.7 nM R-PE | 3554.6 | 0.24 |
| 16.7 nM R-PE | 195.4 | 0.24 |
| 600 nM QD-PEG-NGR | 35689.9 | 0.77 |
| 350 nM QD-PEG | 11457.4 | 0.43 |

Curves for AMP QD and R-PE were compared to develop a direct relationship correlating the numbers of AMP QD and R-PE molecules [Eq. (1)]. Fluorometer instrument settings were chosen to approximate the spectral excitation and emission characteristics of the FACSCalibur flow cytometer used in this study. These measurements confirm that QD fluorescence intensity is large relative to traditional fluorophores. Furthermore, these measurements reveal that surface modification of native AMP QDs significantly modulates fluorescence emission intensity of the QD probes. This modification can be compensated for by the calibration method described here.

marily through specific binding of the NGR peptide to antigens on the cell surface.

Calibration of Fluorescence Data

A linear relationship exists between QD concentration and measured fluorescence intensity. To perform QD binding quantitation, fluorescence measurements were made by both

fluorometry and flow cytometry. Integrated intensities (564–606 nm) of both soluble R-PE and QDs were measured by fluorometry (Table 1). Data was then used to generate standard curves for these molecules relating integrated fluorescence intensity to molecule concentration (Fig. 2A). The linear regression equations were then set equal to one another, producing a standard curve that directly relates AMP QD and R-PE concentrations [Eq. (1)].

$$[\text{QD}] = [\text{PE}] \times 0.2638 - 12.1005 \quad (1)$$

Fluorescence measurements made by flow cytometry were then calibrated to the number of equivalent R-PE molecules using standard calibration microspheres (Fig. 2B). This standard curve was then combined with the fluorometry results to produce a new relationship capable of directly correlating FL2 intensity measured by flow cytometry to the number of equivalent bound AMP QDs [Eq. (2)]. To obtain quantitative binding values for both QD-PEG and QD-PEG-NGR probes, the calculated number of AMP QDs was factored by their measured relative fluorescence to AMP QDs (Table 1).

$$[\text{QD}] = (\text{FL2} \times 438.72 + 1639.8) \times 0.2638 - 12.1005 \quad (2)$$

It is important to note that the particular relationships developed here are valid only for the particular system of fluorophores (AMP QD and R-PE), flow cytometer, and settings used in this calibration. In particular, measurements were conducted on the other two QD species used in this study (QD-PEG and QD-PEG-NGR) as the surface treatments modulate the QD fluorescence quantum yield. This modulated fluorescence behavior essentially created three unique “orphan” fluorophores and resulted in three unique quantitative correlation relationships with the R-PE standards. Unlike the raw fluorescence measurements, the quantitative assessment of the number of QDs associated with each cellular event are absolute values that can be directly compared among the three QD cohorts. The QD per cell results, but not the raw fluorescence

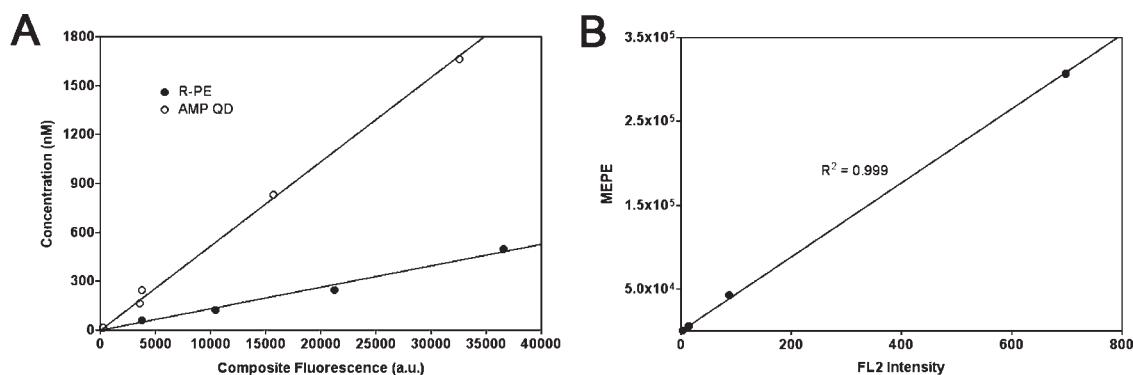


Figure 2. Indirect calibration must be performed to quantitatively analyze fluorophores for which no standards are available. (A) Fluorometry measurements were used to develop standard curves illustrating measured fluorescence as a function of QD or R-PE concentration. These standard curves can be used to determine the relationship between R-PE and QD fluorescence intensity. (B) Flow cytometry fluorescence intensity measurements were translated to the number of equivalent soluble R-PE molecules (MEPE) using commercially available calibration microspheres. Fluorometry and flow cytometry measurements were then combined to develop a direct relationship between flow cytometry fluorescence intensity and the number of equivalent QD probes.

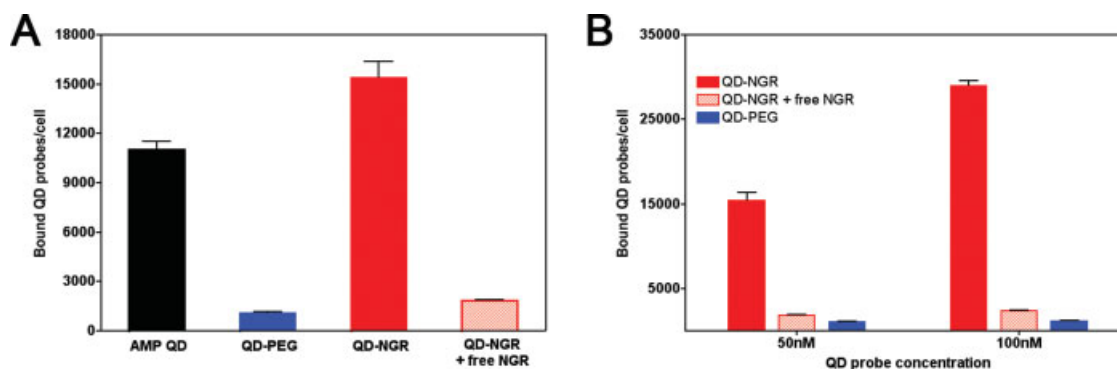


Figure 3. Flow cytometry fluorescence data was calibrated to quantitatively assess QD probe binding to target HT-1080 cells. (A) Surface modification significantly modulates QD interaction with the cell surface. Unmodified AMP QDs exhibit a high level of binding ($11,014 \pm 493$ QD/cell) that can be overcome by surface modification with PEG (1094 ± 64 QD/cell). Addition of the NGR targeting ligand to QD-PEG-NGR results in extensive probe binding to the cell surface ($15,406 \pm 980$ QD/cell). Nearly 90% of this NGR-mediated binding can be inhibited with the addition of a 10-fold excess of free NGR ligand (1867 ± 51 QD/cell). 50 nM QD probe was utilized for all samples; $n \geq 3$ for all cohorts. (B) Increasing probe concentration results in higher levels of QD probe binding. QD-PEG-NGR probe binding nearly doubled to $28,987 \pm 602$ /cell with increased QD concentration. Minor increases in binding were measured at the increased concentration with QD-PEG (1182 ± 58 QD/cell) and QD-PEG-NGR inhibited with free NGR (2390 ± 39 QD/cell). $n \geq 3$ for all experimental cohorts. Bar height is the mean and error bars reflect standard deviation (standard deviation is too low to visualize error bars for QD-PEG-NGR + free NGR and QD-PEG samples on this scale). [Color figure can be viewed in the online issue, which is available at www.interscience.wiley.com.]

intensities, can also be compared to quantitative results from other instruments, settings, and reagents.

Quantitative Measurement of QD Probe Binding to Cells In Vitro

Flow cytometry results, coupled with fluorometer-flow cytometer cross correlation calibration, can be used to determine the number of QD probes bound to the cell surface. The standard curve obtained from the fluorometer-flow cytometer cross calibration was used to relate the FL2 intensity shift of cellular samples to the corresponding number of bound QD probes. The results for each QD surface coating are shown in Figure 3A. Unmodified AMP QDs exhibited significant binding of $11,010 \pm 490$ /cell to the surface of HT-1080 cells. Modification of the QD surface with PEG significantly reduced this interaction to 1090 ± 60 /cell. Addition of the NGR targeting peptide produced the highest cellular interaction of $15,410 \pm 980$ /cell, while introduction of competitive binding with 10-fold excess soluble NGR peptide blocked 88% of binding to 1870 ± 50 /cell. Similar results were seen in experiments utilizing 100 nM QD probes (Fig. 3B).

DISCUSSION

Traditional approaches to disease treatment often involve systemic doses of highly toxic drugs. These approaches are typically limited by nonspecific delivery to nontarget cells, resulting in systemic toxicity (30). Similarly, many imaging reagents are delivered in bolus systemic doses, effectively reducing overall detection sensitivity (by increasing background) or limiting their application to easily accessible compartments (e.g. vasculature). Many prior efforts have focused on targeted delivery of drugs, genes, or imaging agents directly to the target cell type(s) both in vitro (31–33) and in vivo (34–36). However, while offering improvements over nondiscriminant

systemic therapies, many of these approaches suffer from either suboptimal targeting or only a partial quantitative (or even qualitative) analysis of interaction with target sites.

The current study expands on these previous efforts by demonstration of the synthesis and in vitro performance of a versatile, modular nanoscale platform capable of targeted binding, sensing of biological events, and labeling of target cells. Furthermore, we describe a general method for calibration of flow cytometry fluorescence data capable of providing truly quantitative measurements of these constructs and other fluorophores for which appropriate calibration standards are not currently available. This method is implemented here to determine the number of QDs associated with cells in vitro as a function of surface characteristics.

Nanoparticulate systems offer a versatile platform with several distinct advantages in the realm of in vitro and in vivo targeted delivery and detection. Physical characteristics of the nanoparticle base impart features not available with molecular structures alone. These systems provide the opportunity for colocalization of molecular species and the potential for multifunctional capability. Benefits such as these are limited in the absence of a particle, as molecular structures offer lower valency for functionalization and increased likelihood of functional changes following modification. Surface chemistry and three-dimensional particulate structure enable the use of NP systems to provide targeted or localized delivery, to improve bioavailability, to sustain the delivered effect in target tissues, to solubilize agents for intravascular delivery, to improve the stability of therapeutic agents against enzymatic degradation and clearance, and to allow manipulation of the release profile of the delivered therapeutic agent (37). Because of their small physical size, nanoparticles can also penetrate deep into tissues, through fine capillaries, and are generally incorporated efficiently by cells (38).

QDs offer all of the advantages of NP delivery systems previously described with the added benefit of an intrinsic imaging component. The intense fluorescence characteristics of QD probes relative to organic fluorophores facilitates sensitive detection of cell surface interaction not possible with traditional approaches. Furthermore, the spectral characteristics of QD fluorescence lend themselves to the possibility of multiplexed detection of targets. Multiple colors of QD probes can be excited using a single light source while narrow emission bands enable simultaneous detection of multiple different QD colors (corresponding to multiple targets) with minimal crosstalk between detection channels.

Recent publications have examined the toxicity of QDs in both *in vitro* and *in vivo* environments. Some studies have reported that QDs applied to immortalized cell lines *in vitro* result in no significant measures of toxicity (39,40). In primary cultures and *in vivo* applications, possible QD toxicity effects were detected; however, QDs could be rendered nontoxic with appropriate surface coatings (41,42). Long-term degradation of QDs may result in liberation of the core materials of the particle. However, as the studies described here do not occur over these time frames, short-term toxicity studies are expected to be sufficient to predict the response of cultured cells *in vitro*. For *in vivo* applications and long-term studies, toxicity issues associated with QDs and heavy metal release must be considered.

Probe Binding

Our QD probe targeting studies conducted by flow cytometry (Figs. 1B and 3) confirm the dependence of nanoparticle surface modification on cell surface target interaction. PEGylation of the QD surface resulted in a significant decrease in binding over unmodified AMP QDs, with a nearly 90% reduction in nonspecific interaction. This is consistent with previous reports (43–45) detailing the ability of PEG polymers to passivate the surface and minimize undesired interactions with nontarget sites. PEGylated QDs serve as the control for specific binding experiments, as targeted probes are built from the same platform with an added NGR ligand on the distal end of the PEG. Addition of this peptide ligand to the PEG coating mediated a substantial increase in QD binding to the cell surface. Interactions between HT-1080 cells and QD-PEG-NGR increased by 1300% over PEGylated QDs and 40% over unmodified AMP QDs, suggesting significant specific recognition of the NGR targeting ligand by molecules on the cellular surface. These results also follow expected trends for traditional ligand-receptor interaction. Although no specific K_m value is available to describe NGR/CD13 binding, QD-PEG-NGR concentrations used in binding experiments are well below values reported for other peptide-receptor pairs. Thus, QD-PEG-NGR binding is expected to be a function of probe concentration. This behavior is apparent when comparing results for 50 and 100 nM QD-PEG-NGR binding.

Competitive binding experiments were conducted to further examine the specificity of targeted QD probe binding. The addition of a 10-fold excess of free soluble NGR ligand resulted in an 88% inhibition of targeted QD-PEG-NGR

probe binding (100 nM experiments saw a 92% reduction), thus actively reducing binding to levels approaching those of simple QD-PEG probes. Furthermore, the addition of 1% BSA during the binding assay had no effect on QD probe binding (data not shown). These experimental results strongly suggest that increased targeted QD probe binding is a direct result of modification with the NGR targeting peptide, and that this binding is mediated by specific interactions of the NGR peptide with molecules on the cell surface.

While fluorescence intensity measured by flow cytometry indicates functional QD binding to the cell surface and enables “quantitative” comparisons and relative binding levels, these measures are not a direct indication of the number of probes present on the cell surface. Raw measured fluorescence signal is modulated by multiple factors, ranging from the particular fluorophore used to specific instrument settings employed. Thus, direct comparisons of raw fluorescence data are not necessarily accurate indicators of the number of bound probes, especially across multiple systems, instruments, and reagents. To ensure portability and reproducibility, FACS fluorescence intensity data must be correlated to physical values unaffected by experimental conditions.

Calibration

Photomicrographs (Figs. 1C–1F) illustrate considerable modulation of QD probe binding by surface treatment modification. These images support qualitative assessments, but are difficult to employ for quantification of a large sample size, as is available with flow cytometry. Fluorescence intensities measured by flow cytometry have been employed in a number of studies, including the current work, to measure the effects of both passive and active targeting mechanisms (46–48). These approaches provide considerably more information for interpretation and enable simple quantitative comparisons. Nevertheless, fluorescence intensity measurements alone do not support quantitative analysis of probe binding due to a lack of calibration between probe number and fluorescence intensity.

Methods to provide calibrated fluorescence intensities for flow cytometry are limited by the availability of appropriate standards. In many cases, such as with QDs, no commercially available standards currently exist to provide reliable direct calibrations (making these probes “orphan” fluorophores). Ideally, standardized calibration particles would be synthesized for these fluorophores. However, fluorescent nanoparticle probes such as QDs present several yet unresolved obstacles to the synthesis and characterization of any such standards. In these instances, alternative methods must be employed to allow indirect calibration of measured fluorescence data.

The calibration method employed in the current work shares some similarities with the previous body of work on quantitative flow cytometry. As in the current study, many quantitative calculations rely on standardized calibration microsphere sets for conversion of measured fluorescence intensity data to a measure of equivalent fluorophores. These calibration particles can take many forms including standard calibration microsphere sets with fluorophores directly attached to the microsphere surface (27,49), application-speci-

fic microspheres that bind known amounts of fluorophore-labeled proteins such as mAbs (25,29) and other distinct types of fluorescence standards (28). However, the lack of commercially available standards compatible for use with QD probes requires alternate methods.

Studies using some alternate quantification methods similar to the approach described here have appeared previously in the literature (46,50). Like the current work, these studies involve flow cytometry measurement of samples labeled with one fluorophore (e.g. AlexaFluor 488 or Cy3) followed by conversion of the measured fluorescence signal to mean equivalent molecules of a spectrally similar reference fluorophore (e.g. FITC or PE) using a standard calibration microsphere set. These studies then rely on measurement of the relative quantum yield of the experimental and reference fluorophores by fluorometry to convert the final measurement. However, these previous studies base the measurement of relative quantum yield on fluorescence intensity measured at only a single wavelength (535 nm for AlexaFluor488 and FITC, 580 nm for Cy3 and PE). The current study improves on these methods by integrating measured fluorescence (by fluorometry) over the entire range of wavelengths measured by the flow cytometer (i.e. 564–606 nm). This enhancement provides a closer approximation of the true emission response of both probes, rather than basing quantitative measurements on a comparison of fluorescence intensity from a single wavelength.

Accurate calibration of “orphan” fluorophores by the proposed method requires fluorometry measurements using excitation and emission settings that mimic the fluorescence characteristics of the flow cytometer. For example, the FACS-Calibur used in our studies utilizes a single excitation laser (488 nm) while the R-PE and QD fluorophores are maximally detected in the FL2 channel (585/42 nm). Fluorometer settings were chosen to closely approximate these characteristics. Excitation was set to 488 nm (5-nm slit) while the emission intensities were measured from 564 to 606 nm (5-nm slit). Performing these measurements under the same conditions (e.g. pH, buffer components, etc.) minimizes the introduction of error due to environmental modulation of fluorescence.

Another potentially important factor is spectral matching in the choice of fluorescent markers. Ideally, the chosen fluorophores are sufficiently excited by the same laser line and detected by flow cytometry using the same fluorescence channel. This insures sufficient sensitivity for both fluorometry and flow cytometry measurements and minimizes error due to spectral mismatch. However, even with traditional calibration standards, obtaining exact spectral matching between experimental probes and calibration standards across the whole spectrum is difficult, even when using the same fluorochrome, because spectra can shift or broaden depending on how the fluorochrome is attached to the surface of the microbead (28). An additional factor affecting fluorophore selection includes self-quenching, which may be an issue at high concentrations. In our case R-PE was chosen as the calibration fluorophore, as it is very bright and exhibits minimal self-quenching (51). Although R-PE is exceedingly resistant to self-quenching, the behavior of other fluorophores must be carefully considered

when choosing a compatible marker to achieve quantitative results.

It is also important to note that fluorescence characteristics of the chosen probes (i.e. absorption and emission spectra), coupled with optical differences between fluorometer and flow cytometry instrumentation, can contribute to uncertainty in the final quantitative measurements. In the context of the current study, the reference (R-PE) and experimental (QD) probes have different absorption spectra and dependencies on excitation wavelength range and power density. However, excitation of both probes is nearly constant over the 5-nm slit range of the fluorometer. Thus, differences in these spectra should result in little, if any, error in the measurement. Larger uncertainties may be introduced when absorption values of one or both of the chosen probes change dramatically over the excitation wavelength range (~5 nm in this case).

To avoid this source of uncertainty, excitation conditions would be saturating in all cases. As these conditions are not practical in most environments, nonsaturating conditions provide a reasonable approximation. Below saturation (as in most experimental cases), fluorescence intensity is proportional to the product of the molar extinction coefficient and the quantum yield of the individual probes. Thus, at conditions below the saturation point, differences in measured fluorescence intensity between probes in both the fluorometer and flow cytometer should be a function of relative probe concentration, relative molar extinction, and relative quantum yield. As molar extinctions and concentrations are known for both probes (in the fluorometer), and quantum yields remain constant, a simple comparison can be made to determine the relative fluorescence intensity of the probes. However, large inconsistencies in quantitative measurements may become apparent when only one of the probes reaches saturation and the resulting comparison falls outside the linear range.

Emission properties in conjunction with differences in instrument optics must also be considered when choosing appropriate probes. In the current study, the FL2 channel of the flow cytometer is fixed at 585/42 nm while monochromator settings for fluorometer fluorescence are set to 564–606 nm (5-nm slit). The major source of uncertainty in this case occurs at the limits of the measurement range (~564 nm on the low end and ~606 nm on the high end). As emission at these wavelengths represents only a small percentage of the total measured emission profile for both R-PE and QD probes, uncertainty rising from the differences in flow cytometer and fluorometer instrumentation should be minimized (i.e. emission profiles of both probes are very similar across the measurement range and peak emission of both probes occurs at or near 585 nm, the middle of the fluorescence measurement range in both instruments). Fluorescent probes whose emission profiles are less similar or have large changes near the limits of the measurement range may result in greater uncertainty in correlation between the instruments, as edge effects become more prominent for one or both probes.

Once appropriate probes have been chosen and analyzed, the resulting relationship between concentration of the two fluorophores and the measured fluorescence intensities can be

presented as a type of calibration curve that, in this case, is linear (Fig. 2A). This relationship can be used to make a direct comparison between AMP QD and R-PE concentration [Eq. (1)]. Translation of the fluorescence cross-calibration in Figure 2A to quantitative interpretation of flow cytometry data requires a calibrated scale for fluorescence intensity of one fluorophore. Such a calibration is routinely conducted using commercially available reagents (26,27) and appears here as Figure 2B for R-PE. Combining this calculated standard curve with the previously calculated QD to R-PE comparison provides a means for direct conversion of MFI to the number of bound QD probes [Eq. (2)].

By applying the calculated calibration equation [Eq. (2)], we were able to translate fluorescence intensity values as measured by flow cytometry into meaningful measurements of bound QD probes/cell. For targeted therapy or imaging studies, quantitative values such as these can provide important information such as probe binding efficiency, cellular susceptibility to targeted therapy, or toxicity threshold—measurements not possible with traditional uncalibrated flow cytometry techniques. These values are also especially significant for imaging and detection applications, as contrast enhancement and labeling intensity are a direct function of the number or concentration of delivered contrast agents. Furthermore, these calibrated values provide a valuable real-world translation of arbitrary fluorescence values, enabling greater understanding among researchers and data portability among instruments. It is possible that some QDs were removed from the cell surface during cell dissociation, resulting in an artificially low measurement of QD/cell. Thus, the values reported here serve as a lower bound for QD/cell. Any removal of QDs from the cell surface during the cell dissociation protocol would only serve to increase the effectiveness of QD-PEG-NGR conjugates synthesized in this work.

This technique unlocks the underlying power of flow cytometry to allow more detailed quantitative evaluations of probe binding as well as the ability to provide more detailed information on kinetics and efficiency not possible with traditional techniques. For example, measurements from traditional FACS analysis can yield only arbitrary fluorescence increases over time and comparisons between treatments and timepoints. A conversion to quantitative analysis enables these measurements to provide kinetic probe binding values revealing the number of probes bound per time, data which are especially useful for targeted delivery and dosage studies.

Additional analysis can also be performed on the data provided in this study. Fractional binding (total QD added/total QD bound) is nearly identical between 50 and 100 nM samples (0.20 and 0.19%, respectively). These very low values suggest that probe binding has not yet reached saturation at these concentrations and is limited by factors other than QD surface modification. Access to the cell surface is one probable cause, as the colloidal QD probes do not settle during incubation. Furthermore, incubation time (1 h) is sufficiently short to limit significant passive motion of the nanoprobe to the cell surface.

Data on additional probe concentrations and incubation times would enable access to a range of supplementary quantitative characteristics including binding constants, kinetics of saturation, and the number of nanoprobe binding sites, among others. While beyond the scope of the current study, these examples highlight the importance of quantitative data conversion to further analysis of existing FACS measurements.

CONCLUSIONS

We describe the development and performance of a nanoparticle platform capable of targeted binding and delivery, along with a method for providing quantitative performance analysis of this system. This platform offers several distinct advantages over traditional molecular delivery techniques to increase therapeutic efficiency and efficacy while offering a powerful imaging component, especially for *in vitro* analysis. The calibration method developed and employed in this work allows a straightforward conversion of relative fluorescence values into meaningful measurements not affected by experimental conditions. This method extends the capability of quantitative flow cytometry measurements to include fluorescent molecules (e.g. QDs) and fluorophores for which no reliable calibration standards currently exist.

LITERATURE CITED

1. Arap W, Pasqualini R, Ruoslahti E. Cancer treatment by targeted drug delivery to tumor vasculature in a mouse model. *Science* 1998;279:377–380.
2. Pasqualini R, Koivunen E, Ruoslahti E. Alpha v integrins as receptors for tumor targeting by circulating ligands. *Nat Biotechnol* 1997;15:542–546.
3. Pasqualini R, Koivunen E, Kain R, Lahdenranta J, Sakamoto M, Stryhn A, Ashmun RA, Shapiro LH, Arap W, Ruoslahti E. Aminopeptidase N is a receptor for tumor-homing peptides and a target for inhibiting angiogenesis. *Cancer Res* 2000;60:722–727.
4. Curnis F, Arrigoni G, Sacchi A, Fischetti L, Arap W, Pasqualini R, Corti A. Differential binding of drugs containing the NGR motif to CD13 isoforms in tumor vessels, epithelia, and myeloid cells. *Cancer Res* 2002;62:867–874.
5. van Hensbergen Y, Broxterman HJ, Hanemaaijer R, Jorna AS, van Lent NA, Verheul HM, Pinedo HM, Hoekman K. Soluble aminopeptidase N/CD13 in malignant and nonmalignant effusions and intratumoral fluid. *Clin Cancer Res* 2002;8:3747–3754.
6. van Hensbergen Y, Broxterman HJ, Rana S, van Diest PJ, Duyndam MC, Hoekman K, Pinedo HM, Boven E. Reduced growth, increased vascular area, and reduced response to cisplatin in CD13-overexpressing human ovarian cancer xenografts. *Clin Cancer Res* 2004;10:1180–1191.
7. Hallahan D, Geng L, Qu S, Scarfone C, Giorgio T, Donnelly E, Gao X, Clanton J. Integrin-mediated targeting of drug delivery to irradiated tumor blood vessels. *Cancer Cell* 2003;3:63–74.
8. Mamot C, Drummond DC, Greiser U, Hong K, Kirpotin DB, Marks JD, Park JW. Epidermal growth factor receptor (EGFR)-targeted immunoliposomes mediate specific and efficient drug delivery to EGFR- and EGFRvIII-overexpressing tumor cells. *Cancer Res* 2003;63:3154–3161.
9. Oku N, Asai T, Watanabe K, Kuromi K, Ogino K, Taki T. Anti-neovascular therapy by use of liposomes targeted to angiogenic vessels. *J Liposome Res* 2003;13:25–27.
10. Chenavier P, Delord B, Amedee J, Bareille R, Ichas F, Roux D. RGD-functionalized spherulites as targeted vectors captured by adherent cultured cells. *Biochim Biophys Acta* 2002;1593:17–27.
11. Hood JD, Bednarski M, Frausto R, Guccione S, Reisfeld RA, Xiang R, Cheresch DA. Tumor regression by targeted gene delivery to the neovasculature. *Science* 2002;296:2404–2407.
12. Harbottle RP, Cooper RG, Hart SL, Ladhoff A, McKay T, Knight AM, Wagner E, Miller AD, Coutelle C. An RGD-oligolysine peptide: A prototype construct for integrin-mediated gene delivery. *Hum Gene Ther* 1998;9:1037–1047.
13. Hart SL, Collins L, Gustafsson K, Fabre JW. Integrin-mediated transfection with peptides containing arginine-glycine-aspartic acid domains. *Gene Ther* 1997;4:1225–1230.
14. Phadtare S, Vinod VP, Mukhopadhyay K, Kumar A, Rao M, Chaudhari RV, Sastry M. Immobilization and biocatalytic activity of fungal protease on gold nanoparticle-loaded zeolite microspheres. *Biotechnol Bioeng* 2004;85:629–637.
15. Rossi LM, Quach AD, Rosenzweig Z. Glucose oxidase-magnetite nanoparticle bioconjugate for glucose sensing. *Anal Bioanal Chem* 2004;380:606–613.
16. Tang DP, Yuan R, Chai YQ, Zhong X, Liu Y, Dai JY, Zhang LY. Novel potentiometric immunosensor for hepatitis B surface antigen using a gold nanoparticle-based biomolecular immobilization method. *Anal Biochem* 2004;333:345–350.

17. Liu J, Zhang Q, Remsen EE, Wooley KL. Nanostructured materials designed for cell binding and transduction. *Biomacromolecules* 2001;2:362–368.
18. Smith R, Sewell SL, Giorgio TD. Proximity-activated nanoparticles: In vitro performance of specific structural modification by enzymatic cleavage. *Int J Nanomed* 2008;3:95–103.
19. Wang M, Sun C, Wang L, Ji X, Bai Y, Li T, Li J. Electrochemical detection of DNA immobilized on gold colloid particles modified self-assembled monolayer electrode with silver nanoparticle label. *J Pharm Biomed Anal* 2003;33:1117–1125.
20. Zhang D, Chen Y, Chen HY, Xia XH. Silica-nanoparticle-based interface for the enhanced immobilization and sequence-specific detection of DNA. *Anal Bioanal Chem* 2004;379:1025–1030.
21. Alivisatos AP, Gu W, Larabell C. Quantum dots as cellular probes. *Annu Rev Biomed Eng* 2005;7:55–76.
22. Medintz IL, Uyeda HT, Goldman ER, Mattoussi H. Quantum dot bioconjugates for imaging, labelling and sensing. *Nat Mater* 2005;4:435–446.
23. Gerena-Lopez Y, Nolan J, Wang L, Gaigalas A, Schwartz A, Fernandez-Repollet E. Quantification of EGFP expression on Molt-4 T cells using calibration standards. *Cytometry A* 2004;60A:21–28.
24. Schwartz A, Fernandez-Repollet E. Quantitative flow cytometry. *Clin Lab Med* 2001;21:743–761.
25. Smith RA, Giorgio TD. Quantitation and kinetics of CD51 surface receptor expression: Implications for targeted delivery. *Ann Biomed Eng* 2004;32:635–644.
26. Chance JT, Larsen SA, Pope V, Measel JW, Cox DL. Instrument-dependent fluorochrome sensitivity in flow cytometric analyses. *Cytometry* 1995;22:232–242.
27. Iyer SB, Hultin LE, Zawadzki JA, Davis KA, Giorgi JV. Quantitation of CD38 expression using QuantIBRITE beads. *Cytometry* 1998;33:206–212.
28. Schwartz A, Marti GE, Poon R, Gratama JW, Fernandez-Repollet E. Standardizing flow cytometry: A classification system of fluorescence standards used for flow cytometry. *Cytometry* 1998;33:106–114.
29. Zenger VE, Vogt R, Mandy F, Schwartz A, Marti GE. Quantitative flow cytometry: Inter-laboratory variation. *Cytometry* 1998;33:138–145.
30. Frei E. Combination chemotherapy, dose and schedule. In: Holland JF, Frei E III, Bast RC Jr, Kufe DW Jr, Morton DL, Weichselbaum RR, editors. *Cancer Medicine*. 1997. Baltimore, MD: Williams and Wilkins. pp 817–837.
31. Colin M, Maurice M, Trugnan G, Kornprobst M, Harbottle RP, Knight A, Cooper RG, Miller AD, Capeau J, Coutelle C, Brahimi-Horn MC. Cell delivery, intracellular trafficking and expression of an integrin-mediated gene transfer vector in tracheal epithelial cells. *Gene Ther* 2000;7:139–152.
32. Li H, Gray BD, Corbin I, Leberer C, Choi H, Lund-Katz S, Wilson JM, Glickson JD, Zhou R. MR and fluorescent imaging of low-density lipoprotein receptors. *Acad Radiol* 2004;11:1251–1259.
33. Moffatt S, Wiehle S, Cristiano RJ. Tumor-specific gene delivery mediated by a novel peptide-polyethylenimine-DNA polyplex targeting aminopeptidase N/CD13. *Hum Gene Ther* 2005;16:57–67.
34. Adams GP, McCartney JE, Tai MS, Oppermann H, Huston JS, Stafford WF III, Bookman MA, Fand I, Houston LL, Weiner LM. Highly specific in vivo tumor targeting by monovalent and divalent forms of 741F8 anti-c-erbB-2 single-chain Fv. *Cancer Res* 1993;53:4026–4034.
35. Keller G, Schally AV, Gaiser T, Nagy A, Baker B, Halmos G, Engel JB. Receptors for luteinizing hormone releasing hormone expressed on human renal cell carcinomas can be used for targeted chemotherapy with cytotoxic luteinizing hormone releasing hormone analogues. *Clin Cancer Res* 2005;11:5549–5557.
36. Zhao M, Beauregard DA, Loizou L, Davletov B, Brindle KM. Non-invasive detection of apoptosis using magnetic resonance imaging and a targeted contrast agent. *Nat Med* 2001;7:1241–1244.
37. Moghimi SM, Hunter AC, Murray JC. Long-circulating and target-specific nanoparticles: Theory to practice. *Pharmacol Rev* 2001;53:283–318.
38. Vinogradov SV, Bronich TK, Kabanov AV. Nanosized cationic hydrogels for drug delivery: Preparation, properties and interactions with cells. *Adv Drug Deliv Rev* 2002;54:135–147.
39. Jaiswal JK, Mattoussi H, Mauro JM, Simon SM. Long-term multiple color imaging of live cells using quantum dot bioconjugates. *Nat Biotechnol* 2003;21:47–51.
40. Wu X, Liu H, Liu J, Haley KN, Treadway JA, Larson JP, Ge N, Peale F, Bruchez MP. Immunofluorescent labeling of cancer marker Her2 and other cellular targets with semiconductor quantum dots. *Nat Biotechnol* 2003;21:41–46.
41. Derfus A, Chan WCW, Bhatia SN. Probing the cytotoxicity of quantum dots. *Nano Lett* 2004;4:11–18.
42. Hoshino A, Fujioka K Oku T, Suga M, Sasaki YF, Ohta T, Yasuhara M, Suzuki K, Yamamoto K. Physicochemical properties and cellular toxicity of nanocrystal quantum dots depend on their surface modification. *Nano Lett* 2004;4:2163–2169.
43. Akerman ME, Chan WC, Laakkonen P, Bhatia SN, Ruoslahti E. Nanocrystal targeting in vivo. *Proc Natl Acad Sci USA* 2002;99:12617–12621.
44. Ballou B, Lagerholm BC, Ernst LA, Bruchez MP, Waggoner AS. Noninvasive imaging of quantum dots in mice. *Bioconjug Chem* 2004;15:79–86.
45. Gao X, Cui Y, Levenson RM, Chung LW, Nie S. In vivo cancer targeting and imaging with semiconductor quantum dots. *Nat Biotechnol* 2004;22:969–976.
46. James MB, Giorgio TD. Nuclear-associated plasmid, but not cell-associated plasmid, is correlated with transgene expression in cultured mammalian cells. *Mol Ther* 2000;1:339–346.
47. Kunath K, Merdan T, Hegener O, Haberlein H, Kissel T. Integrin targeting using RGD-PEI conjugates for in vitro gene transfer. *J Gene Med* 2003;5:588–599.
48. Nan A, Ghandehari H, Hebert C, Siavash H, Nikitakis N, Reynolds M, Sauk JJ. Water-soluble polymers for targeted drug delivery to human squamous carcinoma of head and neck. *J Drug Target* 2005;13:189–197.
49. Fay SP, Posner RG, Swann WN, Sklar LA. Real-time analysis of the assembly of ligand, receptor, and G protein by quantitative fluorescence flow cytometry. *Biochemistry* 1991;30:5066–5075.
50. Graves SW, Woods TA, Kim H, Nolan JP. Direct fluorescent staining and analysis of proteins on microspheres using CBQCA. *Cytometry A* 2005;65A:50–58.
51. Glazer A. Phycobiliproteins. *Methods Enzymol* 1988;167:291–303.